Eur. Phys. J. A **9**, 385–396 (2000)

THE EUROPEAN PHYSICAL JOURNAL A

Production of neutron-rich isotopes in fission of uranium induced by neutrons of 20 MeV average energy

G. Lhersonneau[1,2,a], P. Dendooven[1], G. Canchel[1,b], J. Huikari[1], P. Jardin[3], A. Jokinen[1], V. Kolhinen[1], C. Lau[4], L. Lebreton[2,c], A.C. Mueller[4], A. Nieminen[1], S. Nummela[1], H. Penttilä[1], K. Peräjärvi[1], Z. Radivojevic[1], V. Rubchenya[1], M.-G. Saint-Laurent[3], W.H. Trzaska[1], D. Vakhtin[5], J. Vervier[2], A.C.C. Villari[3], J.C. Wang[1], and J. Äystö[1,d]

[1] Department of Physics, University of Jyväskylä, POB 35, 40351-Jyväskylä, Finland
[2] Centre de Recherches du Cyclotron, 2 chemin du cyclotron, B-1348-Louvain-La-Neuve, Belgium
[3] GANIL, BP 5027, F-14076 Caen, France
[4] Institut de Physique Nucléaire, F-91406 Orsay, France
[5] Khlopin Radium Institute, St. Peterburg, Russia

Received: 10 July 2000
Communicated by C. Signorini

Abstract. In the context of a parameter study conducted by several laboratories for future European radioactive beam facilities based on fast-neutron induced fission, in particular for the SPIRAL-II project at GANIL, we have measured the yields of neutron-rich isotopes in the mass range of 88 to 144. These nuclei were obtained as fission products of natural uranium bombarded by neutrons of 20 MeV average energy emitted by a thick carbon target irradiated by 50 MeV deuterons. Yields have been measured using on-line mass separation with the ion-guide method. Compared with proton-induced fission at 25 MeV the magnitude of cross-sections, except for the symmetric region, is similar. Z-distributions of isobars have the same width, 0.7 charge units, but their maxima are shifted by about 0.8 charge units, favouring production of the neutron-richer isobars. Our data allow calculations of absolute cross-sections for fission of natural uranium induced by neutrons of about 20 MeV.

PACS. 24.75.+i General properties of fission – 25.85.Ec Neutron-induced fisssion – 25.85.Ge Charged-particle induced fission

1 Introduction

Experiments with radioactive neutron-rich beams are presently a subject of high priority for the nuclear physics community [1–6]. The vast majority of spectroscopic studies of neutron-rich nuclei have been carried out using fission. Numerous decay studies following on-line mass or chemical separation were performed intensively since the seventies [7]. More recently, band properties up to spins typically of 12 $\hbar$ have been investigated with large Ge-detector arrays using spontaneous or heavy-ion–induced fission [8,9].

Generally, neutron-rich nuclei are less known than their neutron-deficient partners at the same distance from the valley of stability. Moreover, there are more neutron-rich nuclei expected to be bound than n-deficient ones. At large neutron excess, a variety of phenomena are predicted such as the existence of neutron skins and vanishing of standard magic numbers.

Yet, one is awaiting for experiments using powerful tools like Coulomb excitation (testing collective properties) and transfer reactions (testing single-particle aspects) to become technically feasible. These should be possible with neutron-rich beams of "reasonable" intensities accelerated to intermediate energies. Another interest for n-rich beams is the synthesis of super-heavy elements. Since the compound nucleus is less neutron deficient than with stable beams, the residual product should be more stable and produced with higher cross-section.

Projects dedicated to acceleration of neutron-rich nuclei to energies above the Coulomb barrier are under development at Oak Ridge (Holifield Radioactive Beam Facility), Argonne National Laboratory in the US and the Munich Fission Fragment Accelerator and SPIRAL-II at

[a] e-mail: lhers@phys.jyu.fi
[b] *Present address*: Institut de Physique Nucléaire, Lyon, IN2P3/CNRS, Université Claude Bernard, F-69622 Villeurbanne Cedex, France
[c] *Present address*: CEA/IPSN, Rue Auguste Lemaire BP6. F-92265, Fontenay aux Roses, France
[d] *Present address*: EP-Division CERN, CH-1211 Geneva 23, Switzerland

GANIL in Europe. The Argonne [10] and SPIRAL-II concepts are based on the use of energetic neutrons produced as a secondary beam to induce fission of natural uranium. In these concepts, energetic neutrons are generated by the interaction of a deuteron beam in a thick target, the so-called converter, in which the deuterons are eventually stopped. A natural uranium target placed close to the converter in the forward direction is exposed to the neutrons. Fission products are obtained by the ISOL (Isotope Separation On-Line) technique [11]. The method has several advantages. The separation of converter and target allows the converter to be cooled and thus to be able to receive very high primary beam intensities. The heated uranium target is bombarded by the secondary neutron beam only. As far as diffusion times are not prohibitive, the U-target size can be made very large to benefit from the high penetrating power of neutrons. Thus, a target of macroscopic dimensions overcomes the intensity losses due to the generation of the neutrons. In contrast to thermal neutrons, energetic particles do not disfavour symmetric fission and open a channel for very asymmetric fission [12, 13]. A larger range of masses is consequently available with reasonable production rates. In addition, compared with proton-induced fission, a shift of the distributions towards more neutron-rich isotopes is expected owing to the larger neutron excess of the fissioning system. Finally, radiation safety problems are less severe than in the vicinity of a nuclear reactor.

The aim of the SPIRAL-II $R\&D$, supported by an European Union RTD contract between the GANIL (Caen), IPN-Orsay, Jyväskylä, KVI-Groningen and Louvain-La-Neuve laboratories, is to investigate the production of neutron beams and measure fission-product yields as function of various design parameters. Choice of converter, best deuteron energy and release characteristics of noble gases from the U-target are the subject of another series of experiments within this contract. There, the PARRNe-I set up [14] has been used and the obtained results will be published elsewhere [15].

Data about nuclide production by neutron-induced fission are extensive for thermal neutrons but, so far, are rather scarce for energetic neutrons. Philips *et al.* reported the most probable mass for a few elements in fission of ^{238}U by neutrons of 2.5 MeV average energy [16].

Several experiments related to production yields in n-induced fission have been performed at Jyväskylä.

Mass distributions of fission products have been measured with part of the HENDES (High Efficiency Neutron DEtection Setup) detectors. A thin uranium target was bombarded by a 65 MeV deuteron beam. Protons emerging after deuteron break-up and both fission fragments were detected in coincidence. By selecting the proton energy, the dependence of mass distributions on neutron energy in the range of 10 to 50 MeV was studied [17].

In another experiment, angular and energy distributions of neutrons generated by stopping a 50 MeV d-beam in a C-converter were measured. Neutrons were detected by 3 position-sensitive neutron detectors covering up to 60 degrees in the forward direction and their energies were measured by time of flight [18]. This experiment defined the properties of the neutron flux used to irradiate the U-target for nuclide yield measurements.

In the present paper, we concentrate on production rates of neutron-rich nuclei. A 50 MeV deuteron beam was delivered by the K-130 cyclotron at Jyväskylä. This energy was chosen since it was also available at the CYCLONE-cyclotron in Louvain-La-Neuve where the release of noble gases from a thick target was studied with the PARRNe1 device. We, therefore, investigate mass ranges that include isotopes of the noble gases Kr and Xe for comparison. This way, it is possible to estimate the release efficiency of these elements in the experiments at Louvain-La-Neuve.

The distribution of nuclidic cross-sections as a function of the atomic number Z within selected isobaric chains are measured at the IGISOL (Ion Guide Isotope Separator On-Line) facility. Absolute cross-section values are subsequently obtained by using the above-mentioned mass-distribution measurements [17] for normalisation. The shape of Z-distributions, *i.e.* width and location of maximum as a function of mass number, will be compared with those for proton-induced fission. Although Kudo *et al.* carried out a systematic study for 24 MeV protons [19], we performed a new experiment with protons at IGISOL to make sure that both measurements of n- and p-induced fission will be analysed in the same way. The results will be compared with a calculation using a model specifically designed for fission [12,13,17] and examples of calculated cross-sections will be shown. Besides the direct application for the SPIRAL $R\&D$, these measurements contribute to the understanding of the fission process. It is getting renewed interest in connection with nuclear waste management and with the advent of new techniques. We note, for instance, the very recent experiments with relativistic secondary heavy-ion beams obtained by fragmentation of 1 GeV/nucleon ^{238}U beams [20].

2 Neutron production

The PARRNe measurements indicate that a carbon converter is the best compromise with respect to deuteron-to-neutron conversion factor and engineering design considerations. Such a converter is used for the experiments described in the following.

The carbon target for converting the deuteron beam into neutrons had a thickness of 1.54 g/cm^2, which is sufficient to stop the 50 MeV deuteron beam inside of it. It was backed by 1.4 mm of steel in order to stop the protons from the deuteron break-up and other created charged particles. The neutron distributions under these conditions [18] are shown in fig. 1. They are in good agreement with those measured by Meulders *et al.* [21]. From these data we calculate deuteron-to-neutron conversion factors (n/d) of about 0.036(4) and 0.035, for refs. [18] and [21], respectively, assuming that all neutrons are emitted in the forward 90 degrees cone in the laboratory.

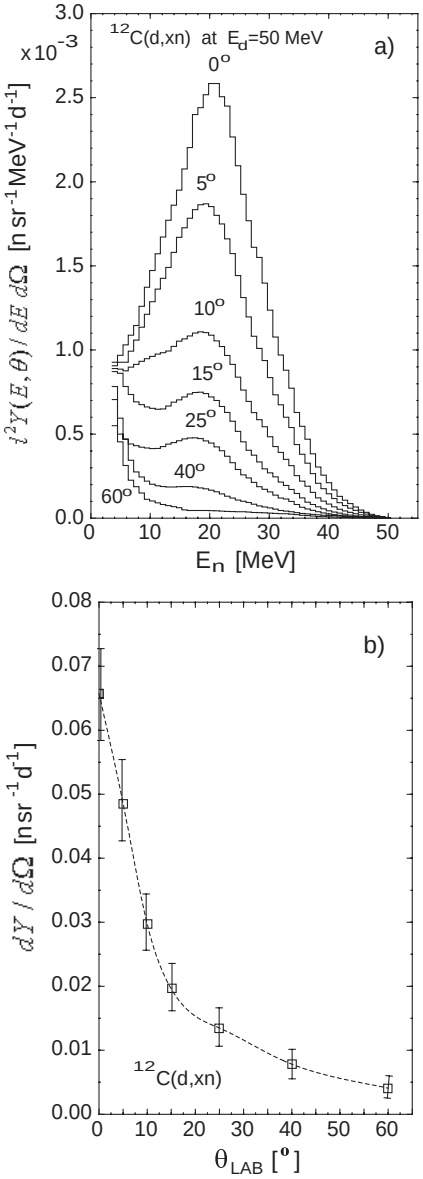

Fig. 1. Neutron distributions measured at HENDES with position-sensitive neutron detectors and under same deuteron energy and converter conditions as the yield and activation measurements [18]. Double-differential and angular (integrated over the energies) distributions are shown on the upper and lower panel, respectively.

In order to obtain an independent measurement of this quantity, we counted γ-rays of activated foils of Al (0.27 g/cm^2) and Co (0.67 g/cm^2) placed downstream of the converter instead of the U-target. They were irradiated for about one hour by the neutrons produced by a deuteron beam of 1.07 μA. Then, they were removed and the residual activity was counted for a period of nearly one week using a 37% coaxial Ge-detector. Firstly, knowing the deuteron beam intensity, activated foil thickness and the measured γ-ray rates one determines a combined experimental cross-section σ_c. Secondly, one can calculate an effective cross-section for neutron activation of the foils,

Table 1. Conversion factor n/d deduced from several reactions of the neutron beam produced by 50 MeV deuterons stopped in a 2 cm thick C-converter. It is obtained as the ratio σ_c/σ_n, see text for these symbols. Note that the quoted values for σ_n and n/d are calculated for neutrons emitted in the 2π forward solid angle, although the foils only actually intercepted a fraction of them. Quoted errors are statistical only.

Reaction	σ_c (mb)	σ_n (mb)	Threshold (MeV)	n/d
^{27}Al(n,p) ^{27}Mg	0.55(2)	19.3	3	0.029(1)
^{27}Al(n,α) ^{24}Na	0.72(3)	23.6	6	0.031(2)
^{59}Co(n,α) ^{56}Mn	0.11(1)	3.4	6	0.032(3)
^{59}Co(n,p) ^{59}Fe	0.24(1)	8.6	4	0.027(2)
^{59}Co(n,2n)^{58}Co	3.4(5)	101	11	0.034(5)

σ_n, which takes into account the angular and energy distributions of the neutrons impinging on the foils. It is obtained by a double integration

$$\sigma_n = \int_\Omega \int_E \{\sigma(E) n(\theta, E)/\cos(\theta)\} \quad \mathrm{d}\Omega \mathrm{d}E$$

where $\sigma(E)$ is the cross-section for the current nucleus at neutron energy E from ref. [22], $n(\theta,E)$ is the double-differential neutron distribution shown in fig. 1, and the factor $1/\cos(\theta)$ corrects for the variation of effective foil thickness with the incident angle. The angular integration has been carried out assuming axial symmetry of the neutron flux. The Al and Co foils intercepted 40% and 24% of the neutrons, respectively, under the approximation that they all were emitted from the center of the converter. Comparison of σ_n with σ_c gives the n/d conversion factor. These quantities are shown in table 1.

The deduced n/d factors for the various reactions are consistent. Thus, the neutron measurements of ref. [18] correctly describe the angular and energy distributions of the neutrons the U-target in the IGISOL measurement was exposed to. The average n/d value is 0.029(3), in which the contribution of the detector absolute efficiency to the uncertainty has been included. It is in fair agreement with the value deduced from independent direct neutron measurements as quoted above [18,21]. We consequently adopt for this C-converter and geometry, when exposed to 50 MeV deuterons a conversion factor n/d of 0.031(4).

We note that according to neutron measurements [23, 24] and simulations [25,26] there is a still room for a subtantial increase of the conversion factor by increasing the deuteron energy.

3 Yield measurements

3.1 Ion-guide set up

The ion-guide technique is well suited for relative cross-section measurements owing to its non-element selective character and fast release time (having allowed the observation of activities with a half-life shorter than 1 ms

[27–30]. Thus, all elements, including refractory ones, can be delivered as beams. Losses due to decay during separation are negligible. The decays of the collected activities are measured by γ-spectroscopy. The only corrections to apply are those due to filiation relationships resulting from β-decay of the isobars during collection, which will be described in section 3.2.

We present here briefly the basic concept of the ion-guide to facilitate understanding of the modifications of its design for neutron-induced fission. We refer to recent status reports for detailed information about the ion-guide [31] and, in particular, the one used for proton-induced fission [32]. The ion-guide method relies on the recoil energy of the reaction products to release them from the target. Thus, the target thickness is limited by the maximum range of these products in the target material. For the fission of uranium or thorium, this is about 15 mg/cm^2. However, since fission fragments are emitted isotropically, it is profitable to tilt the target with respect to the incoming beam direction in order to increase its thickness along the beam path. In our design for p-induced fission, the tilting angle increases the effective thickness by about 6 times. It is also known that the ionization of the helium gas (by the primary beam and recoiling reaction products) results in neutralization through 3-body recombination between the singly charged ions, electrons and neutral helium atoms. These processes, the so-called plasma effect, are responsible for a slower-than-linear increase of the yield with beam intensity. Ionization of the stopping gas by the primary beam can be prevented by placing a thin foil between the target and the stopping chamber.

The actual production rates to be expected in our n-induced fission experiment are of course lower than those for p-induced fission. This is due to at least two factors; first, the practical limit of a few (2–3) μA of the deuteron beam allowed by safety regulations at Jyväskylä (to compare with typically 15 μA for protons, in fact delivered as a H_2^+ beam to increase the number of particles per μA) and, second, the factor of 0.03 times 0.40 for conversion of deuterons into neutrons and the fraction of them emitted in the solid angle viewed by the target (see above). As a result, mass-separated beams below 1 ion/s have to be expected on the wings of the distributions. These intensities are necessarily low since the target must be thin due to the recoil technique IGISOL is based on. For a conventional ISOL method, however, the high penetrating power of neutrons will be effectively used. This will scale up the yields by many orders of magnitude.

In contrast to protons, neutrons are emitted within a rather wide cone. Thus, tilting the uranium target to increase the effective thickness decreases the fraction of neutron beam which can interact with the target. Estimates based on the angular distributions of fig. 1 showed that these contributions roughly cancel. Moreover, charged particles do not enter the ion-guide chamber. There thus is no need for a 2-chamber geometry to reduce the plasma effect. Taking into account these considerations, a new ion-guide chamber for n-induced fission was designed in the hope to increase its efficiency. This lead to the simple chamber shown in fig. 2 where the helium flow near the target has a uniform pattern favourable to efficient transport of the thermalized fission products.

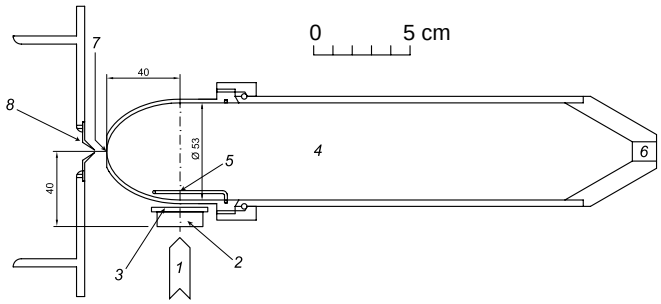

Fig. 2. The ion guide set-up. 1. deuteron beam; 2. 1.54 g/cm^2 carbon converter target; 3. 1.4 mm iron; 4. helium-filled ion guide target chamber; 5. 15 mg/cm^2, 25 mm $\times$ 25 mm ^{238}U target; 6. helium inlet; 7. exit-hole (1.2 mm); 8. skimmer plate with 1.35 mm hole.

Although the ion-guides used for n- and p-induced fission are different, a direct comparison of yields still is possible using the mass distributions measured with HENDES for normalisation [17].

3.2 Measurements and analysis

For each mass to investigate, the measurement consisted of a single irradiation with constant beam intensity. The mass-separated beams were collected on a tape in the focal plane of the separator. During collection the activities were measured with a large coaxial Ge detector (76% relative efficiency) gated by β-particles passing through a thin plastic scintillator. The coincidence was necessary to suppress the natural background which otherwise would have covered the very weak activities of interest. Both β- and γ- energy signals and the time elapsed since the beginning of the collection were recorded as coincidence events with the VENLA multiparameter system [33].

The evolution of transition intensities in the course of irradiation gives access to their half-lives and to the filiation relationships of the isobars. For any nucleus of interest, but the most neutron-rich, β-decay of its parent during collection has to be evaluated in order to extract the rate of incoming ions. Decay half-lives are known and can be regarded as free of errors for the purpose of this experiment. Accordingly, it was only needed to sum all energy-time events along the time axis, analyse the projected energy spectra and apply corrections for the evolution of the activities.

For each observable activity in a given mass chain, peak areas were corrected for detection efficiency and decay branching of the corresponding transitions in order to obtain the number of decays. The set of observed decays belonging to a mass chain can be expressed by a system of linear equations in terms of the unknown production rates. The dimension of the system is the number of nuclei (and their occasional isomers), the activity of which

Table 2. Experimental and fitted cumulative yields in ions/μC of deuteron beam and in 10^3 ions/μC of proton beam. The yields for Kr isotopes and their descendents in the (p,f) run have been corrected as explained in the text. Fitted yields and most probable Z values (calculated from $Z_p(A)= a \cdot A + b$) are for a constant width $\sigma_Z(A)= 0.70$ for both n- and p-induced fission. The accuracy of the $Z_p(A)$ values is better than 0.18 charge units for all listed masses. The parameters $\sigma_Z(A)$, a and b are discussed in the text and shown in tables 3 and 4. Under remarks the factor the experimental yield was multiplied with following renormalisation of ground-state β-branch intensity is occasionally indicated. References for decay data other than [34] are indicated.

A	Z	^{238}U(n,f)			^{238}U(p,f)			remarks
		exper.	fit	$Z_p(A)$	exper.	fit	$Z_p(A)$	
88	34	0.16 (6)	0.07	35.43	0.03 (1)	0.01	36.20	a
	35	0.73 (12)	0.55		0.20 (2)	0.20		b 0.29
	36	0.48 (24)	0.99		0.60 (33)	0.98		
89	35	0.70 (36)	0.41	35.80	0.11 (2)	0.18	36.56	c 0.24
	36	1.20 (20)	1.17		2.51 (33)	1.69		
	37	1.30 (20)	1.36		3.96 (35)	3.41		
90	35	0.80 (30)	0.40	36.17	0.14 (2)	0.09	36.93	
	36	1.80 (40)	2.01		0.94 (33)	1.83		
	37	2.90 (40)	2.86		6.32 (65)	6.00		
91	35			36.53	0.03 (1)	0.02	37.30	d
	36	4.32 (89)	4.59		0.73 (20)	0.91		
	37	9.32 (127)	9.19		5.49 (31)	5.45		
92	36	1.10 (20)	1.16	36.90			37.67	
	37	6.80 (250)	3.77					
93	36	0.40 (10)	0.53	37.27	0.10 (2)	0.09	38.03	
	37	3.65 (51)	3.09		1.99 (16)	2.03		
94	37			37.64	1.57 (15)	0.77	38.40	
	38				4.87 (35)	5.48		
112	43	0.07 (2)	0.08	44.23	0.07 (2)	0.08	45.00	
	44	0.45 (22)	0.41		1.32 (60)	1.84		
	45	1.80 (90)	0.61		6.92 (88)	6.74		e
118	47	0.50 (18)	0.50	46.42				
136	52	2.00 (60)	1.27	53.02	0.28 (4)	0.22	53.81	
	53	4.50 (0)	4.84		1.25 (73)	3.44		f
137	52	0.50 (20)	0.50	53.38	0.03 (1)	0.02	54.18	
	53	5.90 (90)	3.52		1.00 (12)	0.59		g
	54	5.10 (70)	5.95		2.40 (27)	2.89		g
138	53	4.40 (70)	3.49	53.75	0.30 (3)	0.31	54.55	
	54		8.96			2.89		h
	55	8.10(180)	10.17		6.95(140)	5.73		
139	53	1.20 (40)	0.81	54.12	0.05 (2)	0.06	54.91	
	54	4.00 (50)	3.60		0.92 (11)	1.08		
	55	7.20 (280)	4.89		5.10 (210)	3.45		g
	56	4.30 (60)	4.97		7.90 (90)	4.16		g
140	53	0.50 (20)	0.32	54.48	0.02 (1)	0.01	55.28	
	54	1.80 (40)	2.66		0.28 (3)	0.35		
	55	6.60 (80)	4.95		2.17 (15)	2.00		i
141	54	1.00 (30)	1.72	54.85	0.11 (3)	0.21	55.65	j
	55	10.5 (15)	5.07		2.54 (38)	2.34		k
	56	6.80 (60)	5.97		6.09 (48)	5.23		
142	55	5.70 (90)	2.81	55.21	0.56 (8)	0.57	56.01	l 0.61
	56	2.80 (60)	4.10		2.09 (26)	2.14		
	57	5.10 (90)	4.19		2.79 (28)	2.72		m
143	56			55.58	2.11 (24)	2.69	56.38	
	57				6.93 (110)	4.49		
144	55	1.00 (30)	0.46	55.95	0.09 (2)	0.05	56.75	n
	56	1.20 (30)	1.57		1.23 (16)	0.65		
	57	2.10 (30)	1.93		1.27 (18)	1.66		

Table 2. Continued

a)	Yield calculated with g.s. branching of 0.
b)	$\log ft_1 = 9.4$ is assumed instead of the quoted logft = 7.4 (see text).
c)	logft is assumed 6.8 while quoted value is > 5.8.
d)	Branchings from A. Woehr PhD Thesis, Mainz, quoted in [35].
e)	Branchings from [36].
f)	The logft of 8.4 for ^{136}I is fairly high for a first-forbidden transition, the experimental yield could be higher than calculated.
g)	Yield is very sensitive to the large g.s. branching.
h)	Experimental yields are about 3 times less than fits. They are discarded since there is no obvious way to correct them.
i)	The logft of 7.5 for a f-f transition is quite high. Nevertheless, the experimental and fitted yields are in good agreement.
j)	The γ-ray normalisation is unstable due to the allowed character of the g.s. branch, yet the fit is satisfactory.
k)	The large value for n-f is unexplained and was not included in the fit
l)	The logft value of 5.9 is adopted instead of quoted 5.6, see text
m)	The $\log ft_1$ is 10.5. The transition could be faster and the yield higher. The agreement of experiment and fit is nevertheless satisfactory with this value.
n)	The decay scheme of $^{144}Cs^m$ is uncertain.

can be measured with sufficient accuracy. In most cases three different nuclei can be included in the analysis. The coefficients depend on nuclear half-lives and measurement time. They are available from ref. [19]. The solution of these equations is a set of the independent yields of the isobars. Subsequently, these values were added and normalised to form cumulative yields for a beam intensity of 1 μA. This facilitates the identification of inconsistent values on the basis of their deviations with respect to the systematic yield trends *versus* Z and A. The reason for using cumulative rather than independent yields is that they are close to the experimental yields and less correlated. Experimental and cumulative yields merge in the limit of infinitely long measurement times. Furthermore, a questionable cumulative yield can be omitted from the data set without further consequences than losing its value. In contrast, an uncorrect measurement affects the independent yields of the current nucleus and its daughter.

In addition to statistical fluctuations, systematical errors due to erroneous absolute transition intensities per decay contribute to irregularities of the yield pattern versus Z and A. In particular, decays with large ground-state β-feedings should be regarded with caution. A large ground-state branching implies low γ-ray intensities per decay and a high yield. In these cases, a change of ground-state β-branching perhaps meaningless in terms of its logft-value and its physical implications may have dramatic consequences on the deduced yield. As a matter of fact, it has been found necessary to modify a number of ground-state branchings as indicated in the next section.

4 Results

In some cases, the γ-ray intensities per decay as quoted in the table of isotopes [34] indeed lead to several negative independent yields. This occurred as well for the (n,f)-data set as for the, with better statistics, (p,f)-data set. We have assumed that it is due to erroneous ground-state β-branchings. In making readjustments, we have assumed that logft-values for transitions involving the nucleons in the same configurations should vary smoothly. Thus we modified the β-branching intensities accordingly and obtained new decay branchings for the γ-rays. The experimental cumulative yields are listed in table 2. Changes made to decay branchings are clearly indicated so that the original figures can be calculated back if needed.

In order to extract trends out of the data in spite of large fluctuations, fits of cumulative yields have been performed with a restricted number of parameters. The data sets for n- and p-induced fission were always treated separately. In a first step, data were split into sets for the light and heavy mass groups, discarding the few points in the symmetric region. Each set was analysed separately. Z-distributions are conventionally described by Gaussians of width $\sigma_Z(A)$ and centered at $Z_p(A)$. The amplitude, if multiplied with the factor $\sqrt{2\pi}\sigma_Z(A)$, represents the iso-

Table 3. Dependence of χ^2 on the width parameter σ_Z for n-induced fission of ^{238}U. Other parameters, isobaric yields, a and b describing $Z_p(A)$, are free to readjust for each new value of σ_Z. There is a positive correlation between σ_Z and $Z_p(A)$, the latter increasing by 0.9 units over the range of σ_Z values shown here. The number of degrees of freedom is 23.

σ_Z	χ^2	a	b
0.3	117.4	0.374	1.9
0.4	98.3	0.373	2.1
0.5	81.6	0.369	2.7
0.6	73.5	0.368	2.9
0.7	73.6	0.366	3.3
0.8	78.1	0.365	3.5
0.9	84.3	0.365	3.6
1.0	91.0	0.366	3.6
1.1	97.7	0.366	3.7
1.2	103.9	0.366	3.8

Table 4. The local and global fits suggest the same A-dependence of the most probable $Z_p(A)$ over the mass range from 88 to 144. The increase of χ^2 is modest when all points are fitted by a single set of parameters, in spite of the reduction of the number of adjustable parameters and of addition of data in the symmetric region. The $Z_p(A)$ values, shown here at $A = 90$ and 140, remain stable.

Fit of	^{238}U(n,f)			^{238}U(p,f)		
	χ^2	$Z_p(90)$	$Z_p(140)$	χ^2	$Z_p(90)$	$Z_p(140)$
light group	15.0	36.15		67.4	36.90	
heavy group	53.2		54.50	131.1		55.29
sum χ^2	68.2			198.5		
all data	73.6	36.17	54.48	205.2	36.93	55.28

baric yield. Since it is depending on experimental parameters difficult to control, it was left free to vary for each mass. We further assumed that a single $\sigma_Z(A) = \sigma_Z$ parameter and a relation of the type $Z_p(A) = a \cdot A + b$ were sufficient to reproduce the original parameters over the small range of A-values within a mass group.

The $\chi^2(\sigma_Z, a, b)$ values allow a single Z-width parameter for both mass groups. Thus, the best σ_Z value for n-induced fission is 0.65(15), see table 3. It agrees within error bars with the well established value of 0.71(4) for proton-induced fission (this corresponds to the constant $C = 1/\sqrt{2\sigma^2} = 1.00(12)$ quoted in ref. [19]). Since there is no obvious reason for these values to be very different, we adopted a unique value of 0.70 for subsequent fits of both reaction sets.

It was somewhat surprising that we can use a single set of a and b parameters for $Z_p(A)$ for the whole mass range without significant increase of χ^2 compared to a separate treatment for each mass group. Moreover, this applies to both neutron and proton-induced fission, as shown in table 4.

The (a, b) parameters for fits of the whole data sets are (0.3662, 3.21) and (0.3670, 3.90) for n- and p-induced fission, respectively. The deduced most probable $Z_p(A)$ values have respective accuracies of 0.16 and 0.12 in the symmetric region, while becoming a bit smaller (larger) with decreasing (increasing) mass by about 0.02 at the ends of the measured range. A very interesting result is the difference of the offsets, indicating a shift towards larger neutron excess for neutron-induced fission. It is rather stable, as it remains in the range of 0.5 to 1.0 even for large variations of the other parameters.

No parameter has been introduced to take into account an occasional chemical dependence of the ion-guide efficiency. The fair quality of the fits shown above indeed suggests that these effects might be neglected, at least compared with the other experimental uncertainties.

The noble gas Kr, however, seems to be a noticeable exception. The experimental Kr yields follow the general trend in the (n,f) data, but they all appear to be too low in the (p,f) data. This effect is illustrated by the comparison of γ-spectra at mass 91, see fig. 3. During the slowing down of ions in the He-filled chamber charge exchange does not lead to a monotonous decrease of the ionic state until the single-charge state but proceeds back and forth via a number of neutralisations and ionisations. According to the Leuven group [37], these processes might be disturbed by the presence of ionized fission products in the He stopping chamber. This effect is stronger in the p-induced measurements and could tentatively account for the observed losses of Kr isotopes. Nevertheless, a definite explanation for this phenomenon is not available since, in contrast, no such effect was suggested for the other noble gas Xe measured in this work.

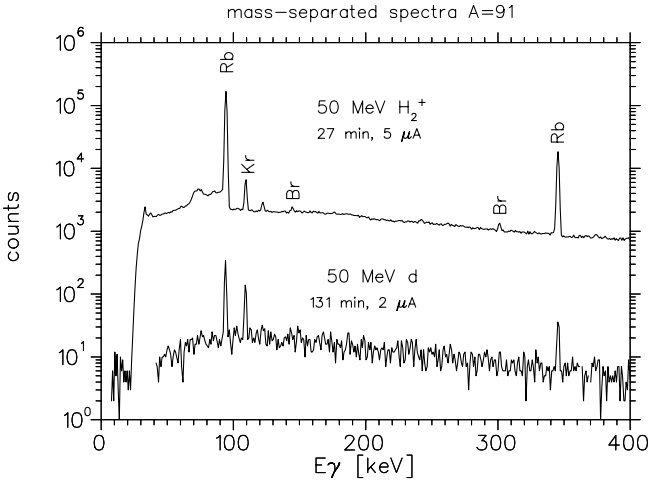

Fig. 3. Gamma-spectra of mass separated $A = 91$ activities. The dramatic drop in the efficiency for Kr with proton beam is clearly visible. The survival of Br activity prevents an arbitrary Z-shift of the maximum of the distribution or a change of the width as alternatives to a lower separation efficiency for Kr.

Assuming the independent Kr yields are suppressed in the (p,f) measurements, a correction factor of 10(2) is required in this case to obtain the best fit. Thus, cumulative yields of Kr isotopes and of their β-decay descendents become larger by 9 times the original independent Kr yields. This correction decreases the χ^2 of the light-group fit by a factor of 6 with respect to the original values. The cumulative yields shown in table 2 include these adjusted values.

A check for consistency of the analysis is the fairly smooth behaviour of the isobaric yields which were treated as free parameters. They are displayed as cross-sections in fig. 4 after a normalisation has been performed to get an overall agreement with the cross-sections extracted from directly measured mass distributions. Cross-sections which are the products of the fission cross-section [38] and probablilities for mass splits [17] are well defined. In con-

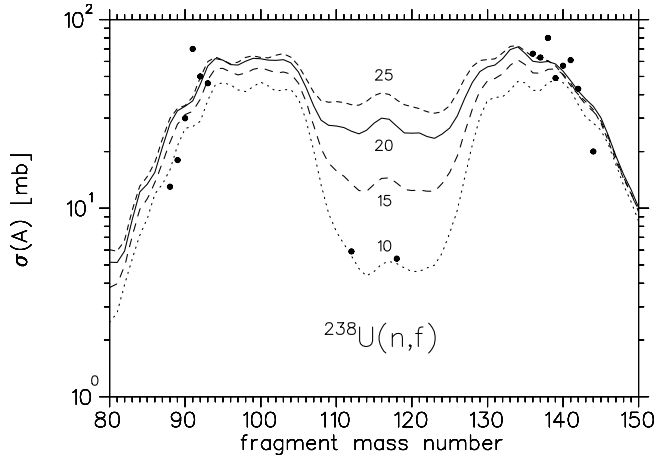

Fig. 4. Cross-sections for isobaric chains in neutron-induced fission. The lines are calculated cross-sections for neutron energies of 10, 15, 20 and 25 MeV which reproduce the values from direct neutron measurements [17] very well. Closed circles are deduced from the isobaric-yield parameters obtained from the fit procedure to extract global trends, see table 2. The original values in ions/μC have been scaled to get an overall agreement with the measured isobaric yields expressed in mb.

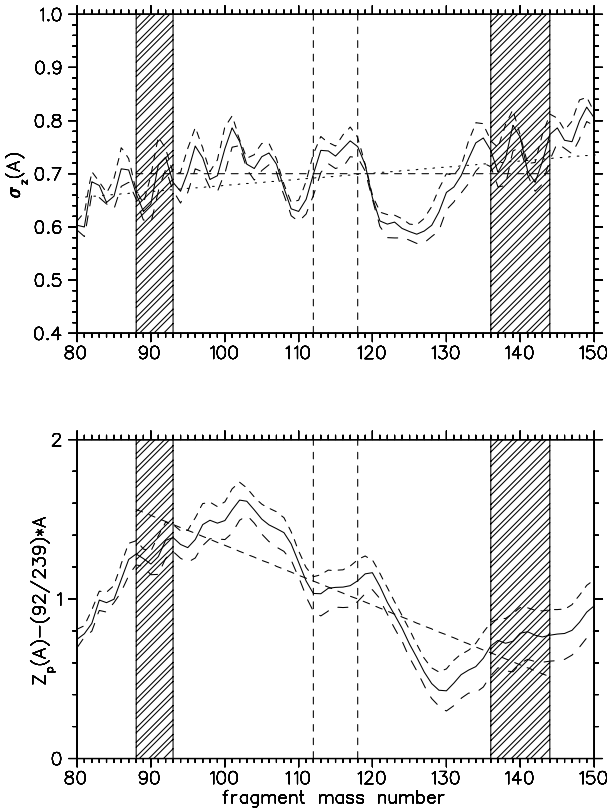

Fig. 5. Calculated and experimental Z-distribution parameters *versus* fragment mass. The oscillating lines are calculated for neutron energies of 15, 20 and 25 MeV, respectively. In both cases, the ordinate is the largest for the higher energy. Hatched areas and vertical lines show the masses measured in this work. Top: Width parameter of the charge distribution. The general trend of calculated values is given by the dotted line defined as $\sigma_Z = 0.70 + 0.0012(A - 120)$, which is in good agreement with the adopted constant of 0.70 shown as a dashed line. Bottom: Most probable charge Z_p plotted as residual after subtracting the UCD value. The straight line shows the parametrisation given in the text, $Z_p(A) = 0.3662 \cdot A + 3.21$. Its uncertainty is less than 0.2 charge units in the measured mass range.

trast, the normalisation of our isobaric yields contains an empirical scale factor due to the efficiency of the IGISOL mass separator. The general trend follows the shape of experimental (directly measured) and calculated mass distributions. The large scattering of some values should be due to varying experimental conditions rather than have a physical meaning.

We note that the valley in the symmetric region remains with a peak-to-valley (P/V) ratio of about 10. It is, as expected, much more shallow than for thermal-neutron induced fission of ^{235}U where P/V is about 600 [39]. Nevertheless, our P/V is larger than that reported by Zöller who used a neutron beam at Los Alamos (about 3.5 for a neutron-energy bin of 18–22 MeV) [40] and the HENDES group (2.8) [17] using deuteron break-up. We note that the neutron measurements, see fig. 1, show an increase of the neutron flux at low energies. The rather isotropic distribution of these low-energy neutrons suggests another mechanism than stripping, possibly evaporation from the target nucleus. Part of these neutrons are probably not observed due to the detection threshold of 3 MeV. Even a small amount of them could increase the P/V ratio which varies rapidly at this energy [40,41].

5 Discussion

We have searched for global trends of the Z-distributions measured for isobaric chains in the $A = 90$ and $A = 140$ regions. Our results indicate a width parameter σ_Z of 0.65(15). The data do not allow a definite claim for its dependence on mass number. The calculations shown in fig. 5 display a slightly increasing trend represented by the function $\sigma_Z = 0.70 + 0.0012(A - 120)$ in good agreement with the experiment. It can be assumed that the widths for n- and p-induced fission are the same, namely $\sigma_Z = 0.70$. The most probable Z_p-values extracted from experiment were constrained by a linear dependence on the mass. An unexpected result is that the same set of coefficients a and b could be used for both mass regions. In the experimental mass range, the linear trend is globaly reproduced by the calculation, but the calculated values show oscillations leading to deviations of up to 0.4 charge units with respect to the experimental line with $Z_p(A) = 0.3662 \cdot A + 3.21$, see fig. 5. Moreover, the deviations increase rapidly outside of the measured region, becoming larger than the experimental accuracy of 0.2 charge units. For instance, compared with the extrapolated linear function, the calculation turns out to shift the distributions of light neutron-rich nuclei towards the most neutron-rich isobars. It would be interesting to get experimental points outside of the measured range in order to test the predictive power of the calculation or/and of

Table 5. Most probable mass for elements observed in fission of ^{238}U at two average neutron energies, from this work and ref. [16].

Element	$A_p(Z)$			Exper. shift
	20 MeV		2.5 MeV	
	exper.	theory	ref. [16]	
$_{40}$Zr	100.5 (4)	99.9	101.60 (9)	1.1
$_{52}$Te	133.2 (5)	133.7	135.41 (9)	2.2
$_{54}$Xe	138.7 (5)	138.0	140.16 (16)	1.5
$_{56}$Ba	144.2 (5)	142.8	144.81 (14)	0.6

the experimental parametrisation. This, unfortunately, requires under present experimental conditions prohibitive measurement times due to the rapidly decreasing cross-sections. The calculation also predicts a modest width dependence and fine structure of the most probable Z-values as a function of A. The experimental accuracy is, however, too limited to definitely confirm this effects.

It is interesting to compare our data with those published recently for neutrons of 2.5 MeV average energy [16]. The most probable masses by Philips *et al.* [16] and our calculated ones (rewriting our equation for $Z_p(A)$ as $A_p(Z) = 2.730Z - 8.8$) are shown in table 5. They indicate loss of about 1.4 neutrons on the average when increasing the average energy from 2.5 MeV to 20 MeV in our experiment. This is probably due to evaporation of a larger number of neutrons at higher excitation energies. According to calculations in ref. [40], there are no pre-fission neutrons at the lowest energy but 1.17 on the average at 20 MeV, whereas the number of post-fission neutrons increase from 1.52 to 1.93. Thus, the calculated value is 1.58, in good agreement with our observations. Keeping in mind production of neutron-rich nuclei in future radioactive beam facilities, it is therefore of importance to consider carefully the best energy with respect to overall production, filling of the valley in the symmetric region and position of the maximum of the Z-distributions.

It is also interesting to compare our results for proton-induced fission with the systematic study of Kudo *et al.* [19]. We have used the same width parameter σ_Z of 0.70 as in their work. By construction, our Z_p values steadily increase with mass number. Kudo *et al.*, however, use another formalism in order to cancel chemical effects in the ion-guide. Their method produces large fluctuations and it can hardly be exploited in case of weak statistics. They report backwards-going Z_p values at masses 88 and 142. This behaviour is caused apparently by the different spectroscopic input for these masses, as suggested by our new evaluation of ground-state β-branchings. We have assumed for ^{88}Br a 2^- ground state, and adopted for the resulting first-forbidden (ff) unique branch to ^{88}Kr a $\log ft_1$ value of 9.4 derived from the local systematics of $2^- \rightarrow 0^+$ transitions. (We note that for a ff-unique transition $\log ft_1 = \log ft + 1.08$.) For the mass 142, our evaluation results in the increase of the anomalously low logft value of 5.6 for the ff-transition from ^{142}Cs to the ^{142}Ba ground state [42]. We reduced the β-feeding by a factor of 2, thus raising the logft value to 5.9 that is the generally adopted lower limit for such a transition. With these quite reasonable changes, the data come closer to the average trend and there is no need to decrease the Z_p values locally. Thus, it might not be necessary to invoke a nuclear structure effect as proposed in ref. [19].

The general trends in both works yet are similar. Both show smaller $\mathrm{d}Z_p(A)/\mathrm{d}A$ slopes than the UCD value (unchanged charge distribution) of $Z/A = 93/237 = 0.392$, assuming the fissioning nucleus to be ^{237}Np. From the data of Kudo *et al.* we estimate an average trend of $Z_p - Z_{\mathrm{UCD}} = 0.0325(A' - 120)$, with $A' = A + 2$. The corresponding calculated $Z_p(A)$ values for $A = 90$ and 140 are 37.0 and 55.0, while ours are 36.93 and 55.28 (table 2), respectively. In conclusion, there is at least good global agreement between their and our works.

Finally, our (n,f) results indicate a nearly constant shift of the Z-distributions in the range $A = 88$ to $A = 144$ towards the neutron-rich side with respect to proton-induced fission. Its value of 0.8 charge units seems rather large. Intuitively, from the above $(Z/A)_{\mathrm{UCD}}$ equation, one would expect a variation about 0.5 units. This difference of 0.3 units represents a 1.5 standard deviation of the typical Z_p(n,f)-Z_p(p,f) shifts as obtained from the fits. A shift of $\Delta Z_p = 0.5$ can be obtained as the best χ^2 solution from our data (the distribution for proton-induced fission still being fitted with the width of 0.70) only for a σ_Z value larger than 1.0 and at the expense of a large increase of chi-square, see table 3. The existence of a sizeable shift is thus clear. As a consequence, it might be of interest to consider (fast) neutron-induced fission for investigations of the most n-rich nuclei, provided that very intense primary beams and appropriate converters can be made and thick targets with sufficiently short release times can indeed be developed.

The present data have a most direct application in enabling calculation of production rates for isotopes until now impossible to measure, if the yields of their neighbours are known. For example, noble gases are used to study design parameters with the PARRNe device. Thus, it is possible to predict the amount of halogens produced in the U-target and how much they influence yield and release-time measurements of rare gases by their decay. We present ^{238}U(n,f) and ^{238}U(p,f) cross-sections for some elements of technical interest in fig. 6.

6 Conclusion

We have measured production rates for nuclei in the light and heavy fission groups using a secondary n-beam produced by stopping a 50 MeV d-beam in a 1.54 g/cm^2 C-converter. The conversion factor of deuterons into neutrons has been found to be near 3% in our experimental conditions. Yield measurements using mass separation with the non Z-selective ion-guide technique have given the distribution of cross-sections *versus* Z in the selected mass chains. The first result is that the Z-distributions are well fitted with a constant width, σ_Z=0.7. This value is identical to the one adopted for fission induced by protons

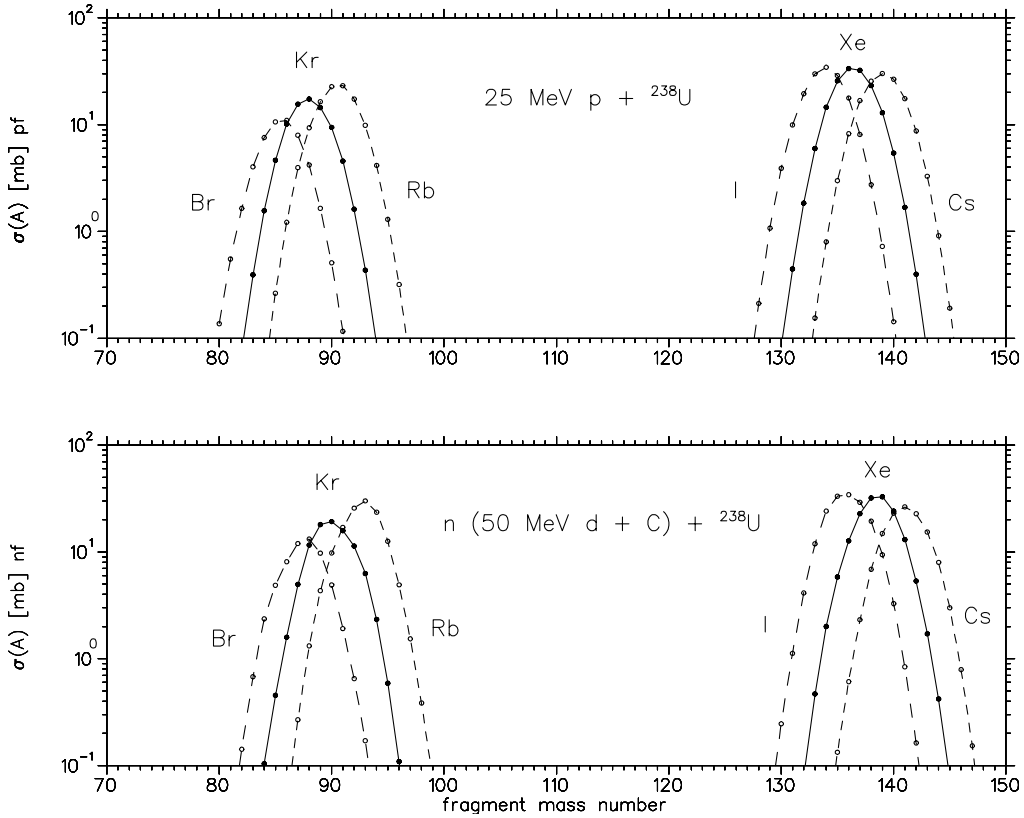

Fig. 6. Calculated cross-sections for some elements of practical interest in the testing phase of the SPIRAL *R&D*. Shown are Br, Kr, and Rb on the left-hand side and I, Xe and Cs on the right-hand side. The values (dots) are obtained by combining mass yields shown on figure 4 and Z-distributions of isobars calculated from the parametrisation described in the text. Curves are a guide to the eye only. Note the shift between the top of the mass distributions for 25 MeV protons (top) and for the neutrons generated by 50 MeV deuterons on the C-converter (bottom).

of intermediate energy. A second result is the linear dependence of the most probable $Z_p(A)$ values over a wide mass range spanning the $A = 90$ and $A = 140$ mass regions. These features are globally reproduced by model calculations. However, outside of the measured range, the most probable $Z_p(A)$ values start to diverge. Finally, there is a shift of the distributions towards a larger neutron excess with respect to proton-induced fission at 25 MeV, favouring production of the most neutron-rich nuclei. The n/d conversion factor is overcompensated on the wings of the distributions for $Z(A) < Z_p(A) - 2$. The absolute yields show a valley in the symmetric region. It is somewhat deeper in our results using mass separation ($P/V = 10$) than in direct measurements of fission fragments. A definite explanation for this discrepancy has not been found. The presence of an intense low-energy neutron distribution below the threshold of neutron detection might be invoked.

By combining our Z-distribution measurements with isobaric yield cross-sections, one easily obtains absolute cross-sections for products of fission induced by intermediate-energy (centered near 20 MeV) neutrons.

As a conclusion, these data will be useful for further development of the SPIRAL-II project and, more generally, for the improvement of the theoretical understanding of fast-neutron–induced fission.

The research and development of SPIRAL-phase II is supported by european programs under the contract number ERBFMGECT980100. This work was supported by the Access to Large Scale Facilities program under the Training and Mobility of Researchers program of the European Union.

References

1. *Nuclear Science A Long Range Plan*, The DOE/NSF Nuclear Science Advisory Committee, USA Department of Energy and National Science Foundation (USA, Feb. 1996).
2. *Scientific Opportunities with the advanced ISOL Facility*, the 'Columbus' White Paper (USA, Nov. 1997).
3. *Nuclear Physics in Europe, Highlights and Opportunities*, Report from the Nuclear Physics European Collaboration Committee (Europe, Dec. 1997).
4. *Proposal for Japan Hadron Facility*, High-Energy Accelerator Research Organisation (KEK), JHF Project Office (Japan, April 1997).
5. *Report of the Study Group on Radioactive Nuclear Beams*, OECD Megascience Forum (OECD, February 1999).

6. The NuPECC Working Group on Radioactive Nuclear Beam Facilities (Europe, April 2000).
7. See, *e.g., Proceedings of Conference on Exotic Nuclei and Nuclear Masses, Bellaire, Michigan, USA, 1998*, edited by B.M. Sherill, D.J. Morissey and C.N. Davids, *AIP Conf. Proc.* **455**, (AIP Publishing, Woodbury, New York, 1998).
8. J.H. Hamilton, A.V. Ramayya, S.J. Zhu, G.M. Ter-Akopian, Yu. Oganessian, J.D. Cole, J.O. Rasmussen and M.A. Stoyer Progr. Part. Nucl. Phys. **35**, 635 (1995).
9. M.G. Porquet, in *Proceedings of the 2nd International Conference On Fission and Neutron-Rich Nuclei, St. Andrews, Scotland, 1999*, edited by J.H. Hamilton, W.R. Phillips and H.K. Carter, (World Scientific, Singapore, 2000) p. 116.
10. J. Nolen, *Proceedings of the 3rd International Conference On Radioactive Nuclear Beams, East Lansing, Michigan, USA*, May 24-27, 1993, edited by D.J. Morrisey, (Editions Frontières, Gif sur Yvette, 1993) p. 111.
11. H.L. Ravn and B. Allardyce, in *Treatise of Heavy-Ion Science* edited by D. Allan Bromley, Vol. 8 (Plenum Press, New York 1989).
12. P.P. Jauho, A. Jokinen, M. Leino, J.M. Parmonen, H. Penttilä, J. Äystö, K. Eskola and V.A. Rubchenya, Phys. Rev. C **49**, 2036 (1994).
13. M. Huhta, P. Dendooven, A. Honkanen, A. Jokinen, G. Lhersonneau, M. Oinonen, H. Penttilä, K. Peräjärvi, V.A. Rubchenya and J. Äystö, Phys. Lett. B **405**, 230 (1997).
14. F. Clapier, A.C. Mueller, J. Obert, O. Bajeat, M. Ducourtieux, A. Ferro, A. Horbowa, L. Kotfila, C. Lau, H. Lefert, S. Kandri-Rody, N. Pauwels, J.C. Potier, J. Proust, J.C. Puteaux, C.F. Liang, P. Paris, A.C.C. Villari, R. Lichtenthäler, L. Maunoury, J. Lettry, Phys. Rev. Special Topics-Accelerators and Beams **1**, 013501 (1998).
15. F. Ibrahim et al., IPN-Orsay Annual Report 1998-1999, 21 (2000).
16. W.R. Philips, A.P. Byrne, G.D. Dracoulis, G.J. Lane, T.R. McGoram, and R. Newman, Eur. Phys. J.A **3**, 205 (1998).
17. V.A. Rubchenya, J. Äystö, P. Dendooven, S. Hankonen, A. Jokinen, W.H. Trzaska, D.N. Vakhtin, J.C. Wang, A.V. Evsenin, S.V. Khlebnikov, A.V. Kuznetsov, V.G. Lyapin, O.I. Osetrov, G.P. Tiourin, A.A. Alexksandrov and Yu.E. Penionzhkevich, in *Proceedings of the 2nd International Workshop on Nuclear Fission and Fission-Product Spectroscopy, Seyssins, France, 1998* , edited by G. Fioni, H. Faust, S. Oberstedt and F.J. Hambsch, *AIP Conf. Proc.* **447**, (AIP Publishing, Woodbury, New York, 1998) p.453; V.A. Rubchenya, A.A. Alexandrov, I.D. Alkhazov, J. Äystö, K.-T. Brinkmann, A. Evsenin, S.V. Khlebnikov, A.V. Kuznetsov, V.G. Lyapin, M. Mutterer, Yu.E. Penionzhkevich, O.I. Osetrov, Z. Radivojevič, M.-G. Saint-Laurent, Yu.G. Sobolev, G.P. Tjurin, W.H. Trzaska, D.N. Vakhtin, in *Proceedings of the 2nd International Conference On Fission and Neutron-rich Nuclei, St. Andrews, Scotland, 1999*, edited by J.H. Hamilton, W.R. Phillips and H.K. Carter, (World Scientific, Singapore, 2000) p. 484.
18. Z. Radivojevič, D. Vakhtin, A. Honkanen, V. Lyapin, W.H. Trzaska and J. Äystö, JYFL Ann. Rep. (1999) and submitted to Nucl. Instrum. Meth. Phys. Res. A.
19. H. Kudo, M. Maruyama, T. Tanikawa, T. Shinozuka and M. Fujioka, Phys. Rev. C **57**, 178 (1998).
20. K.-H.Schmidt, S. Steinhäuser, C. Böckstiegel, A. Grewe, A. Heinz, A.R. Junghans, J. Benlliure, H.-G. Clerc, M. de Jong, J. Müller, M. Pfützner and B. Voss, Nucl. Phys. A **665**, 221 (2000).
21. J.P. Meulders, P. Leleux, P.C. Macq and C. Pirart, Phys. Med. Biol. **20**, 235 (1975).
22. ENDF/B-V Data for Fission Products and Actinides, EPRI-NP-3787, Project 975-2, LA-UR 83-1285, ENDF-322, Los Alamos National Laboratory (1984).
23. S. Ménard, M. Mirea, F. Clapier, N. Pauwels, J. Proust, C. Donzaud, D. Guillemaud-Mueller, I. Lhenry, A.C. Mueller, J.A. Scarpaci and O. Sorlin, Phys. Rev. Special Topics - Accelerators and Beams **2**, 033501 (1999).
24. N. Pauwels, F. Clapier, P. Gara, M. Mirea and J. Proust, Nucl. Instrum. Methods Phys. Res. B **160**, 315 (2000).
25. D. Ridikas, PhD thesis, GANIL report GANIL-T-99-04 (October 1999).
26. D. Ridikas and W. Mittig, in *Proceedings of Conference on Exotic Nuclei and Nuclear Masses, Bellaire, Michigan, USA, 1998*, edited by B.M. Sherill, D.J. Morissey and C.N. Davids, *AIP Conf. Proc.* **455**, (AIP Publishing, Woodbury, New York, 1998) p. 1003.
27. J. Äystö, P. Taskinen, M. Yoshii, J. Honkanen, P. Jauho, J. Ärje, and K. Valli, Nucl. Instrum. Meth. Phys. Res. B **26**, 394 (1987).
28. P. Taskinen, H. Penttilä, J. Äystö, P. Dendooven, P. Jauho, A. Jokinen, and M. Yoshii, Nucl. Instrum. Meth. Phys. Res. A **281**, 539 (1989).
29. J. Äystö, Nucl. Instrum. Meth. Phys. Res. B **40/41**, 489 (1989).
30. P. Dendooven, in *Proceedings of the EMIS-13 Conference, Bad Dürkheim, Germany, 1996*, Nucl. Instrum. Methods Phys. Res. B **126**, 182 (1997).
31. H. Penttilä, P. Dendooven, A. Honkanen, M. Huhta, G. Lhersonneau, M. Oinonen, J.M. Parmonen, K. Peräjärvi and J. Äystö, in *Proceedings of the EMIS-13 Conference, Bad Dürkheim, Germany, 1996*, Nucl. Instrum. Methods Phys. Res. B **126**, 213 (1997).
32. P. Dendooven, S. Hankonen, A. Honkanen, M. Huhta, J. Huikari, A. Jokinen, V.S. Kolhinen, G. Lhersonneau, A. Nieminen, M. Oinonen, H. Penttilä, K. Peräjärvi, J.C. Wang and J. Äystö, in *Proceedings of the 2nd International Workshop on Nuclear Fission and Fission-Product Spectroscopy, Seyssins, France, 1998*, edited by G. Fioni, H. Faust, S. Oberstedt and F.J. Hambsch, *AIP Conf. Proc.* **447**, (AIP Publishing, Woodbury, New York, 1998) p. 135.
33. K. Jääskeläinen, P.M. Jones, A. Lampinen, K. Loberg and W. Trzaska, JYFL Annual Report 1995, (1996) p. 15.
34. R.B. Firestone, *Table of Isotopes*, 8th ed. (John Wiley and Sons, New York, 1996).
35. A. Woehr, PhD University of Mainz, Germany (1992). quoted in C.M. Baglin, Nucl. Data Sheets **86**, 1 (1999).
36. G. Lhersonneau, J.C. Wang, S. Hankonen, P. Dendooven, P. Jones, R. Julin and J. Äystö, Phys. Rev. C **60**, 014315-1 (1999).
37. P. van Duppen and M. Huyse, IKS Leuven, Belgium, private communication.
38. V.P. Eismont, A.P. Korobkin, A.V. Prokofyev, A.N. Smirnov, J. Blomgren, H. Conde, K. Elmgren, N. Olsson, J. Rahm, E. Ramstrom, in *Proceedings of International Conference on Nuclear Data for Science and Technology, Trieste, Italy, 1997*, edited by G. Reffo, A. Ventura, C. Grandi, (Editrice Compositori, Italy, 1997) p. 494.

39. A.C. Wahl, At. Data Nucl. Tables, **39**, 1 (1988).
40. C.M. Zöller, PhD , Technical Hochschule Darmstadt, Germany (1995).
41. F. Vives, F.J. Hambsch, H. Bax and S. Oberstedt Nucl. Phys. A **662**, 63 (2000).
42. B. Singh, J.L. Rodriguez, S.S.M. Wong and J.K. Tuli Nucl. Data Sheets **84**, 487 (1998).